

Observation of Spontaneous Self-Channeling of Light in Air below the Collapse Threshold

C. Ruiz, J. San Román, C. Méndez, V. Díaz, L. Plaja, I. Arias, and L. Roso

Departamento de Física Aplicada, Universidad de Salamanca, E-37008 Salamanca, Spain

(Received 1 September 2004; published 29 July 2005)

We report the observation of the self-guided propagation of 120 fs, 0.56 mJ infrared radiation in air for distances greater than 1 m. In contrast with the known case of filamentation, in the present experiment the laser power is lower than the collapse threshold. Therefore the counterbalance between Kerr self-focusing and ionization induced defocusing as the stabilizing mechanism is ruled out. Instead, we find evidence of a process in which the transversal beam distribution reshapes into a form similar to a Townes soliton, with the particularity of a very high stability. We include numerical support for this conclusion.

DOI: [10.1103/PhysRevLett.95.053905](https://doi.org/10.1103/PhysRevLett.95.053905)

PACS numbers: 42.65.Tg, 05.45.Yv, 42.65.Jx

Spontaneous guiding of intense femtosecond laser beams is a relevant consequence of propagation in non-linear media. It was first observed by Braun *et al.* [1] in the form of light filaments extending over a distance of 20 meters. This triggered an intense experimental and theoretical research to better understand the underlying mechanism as well as to develop practical applications of the phenomena. Fundamentally, the light channels appear in situations in which a compromise between collapse and expansion of the transversal beam profile is possible. In the most known case, self-channeling at high laser powers, these opposite trends come from the self-focusing effect in Kerr media and the dispersion induced by the inhomogeneous refractive index resulting from ionization [2]. In this case, a filament of light can be spontaneously formed when the self-focusing is strong enough to produce the collapse of the beam. The increased intensity in the focus produces ionization and, thus, a change in the refraction index that counterbalances the Kerr focusing. However, this mechanism is not unique. In this Letter we report the observation of this sort of structures for intensities below the critical power of collapse. For this case, ionization does not play a relevant role, and the counteracting mechanism combines the focusing power of the Kerr effect with the beam diffraction. Including an estimation of the retardation effects of the dispersive medium by the computation of the corresponding integral [3], the propagation of the laser beam can be described by a nonlinear Schrödinger equation in the transverse coordinates. In particular, for the cylindrical symmetric case we have

$$i \frac{\partial}{\partial z} U(r, z, t) = -\frac{1}{2k_0} \left[\frac{\partial^2}{\partial r^2} + \frac{1}{r} \frac{\partial}{\partial r} \right] U(r, z, t) - \frac{k_0 n_2}{2} |U(r, z, t)|^2 U(r, z, t), \quad (1)$$

where k_0 is the wave vector of the laser radiation and n_2 is the nonlinear refraction index (3.2×10^{-19} cm²/W). Note that Eq. (1) is derived according to the slowly varying envelope approximation (SVEA) [4]. As a result, the temporal coordinate factorizes and every time slice of the electromagnetic pulse evolves independently. $U(r, z, t)$ is

defined as the time dependent field envelope $U_0 g(r, z, t)$, so that $U_0^2 = E_{\text{in}}/V$ with $V = \int r dr dz dt |g(r, z, t)|^2$, E_{in} being the input energy of the beam. A singular aspect of Eq. (1) is the possibility of localized self-trapped solutions, or solitons. In particular, the so-called Townes soliton [5]. This kind of solution reflects situations in which diffraction is counterbalanced by self-focusing and, therefore, represents transversal self-trapping of a portion of the laser beam. The observation of such structure generated after the propagation of an infrared beam through 30 cm of BK7 glass has already been reported in [6]. However, the stability of this structure was not investigated. This is an important point, since the Townes solution is known to be unstable under small energy fluctuations of the trapped field [7]. The instability leads to the destruction of the self-trapping in the form of a catastrophic collapse or the transversal spread of the beam. Under these circumstances, the extension of the light channel in experiments depends strongly on the degree of approximation to the actual soliton shape. In this Letter we report, on one side, the first observation of the Townes profile in air. On the other side, we report the stability of the self-trapped channel over more than 1.5 m (about 31 Rayleigh lengths). Considering the unstable nature of this type of soliton, it is important to point out that our finding is specially relevant due to the random inhomogeneities of the propagating medium. In addition, the observed shot-to-shot stability of the soliton profile provides a further indication of the robustness of this solution against different configurations of the medium coming from fluctuations in time. This high stability situation opens new interesting possibilities. For instance, this type of channel of radiation can be optically manipulated [8] in order to investigate the interaction of such structures or, even more interesting, they can be used as the input of further devices.

Figure 1 shows schematically the experimental setup employed in this experiment. A 120 fs, 790 nm Ti:Sa laser pulse (1 cm transversal FWHM) is focussed in air with a 2.2 m focal lens, right after passing through the aperture (radius 0.25 cm). A BK7 plate, located at a variable distance from the focal spot, is used to intercept the beam. The

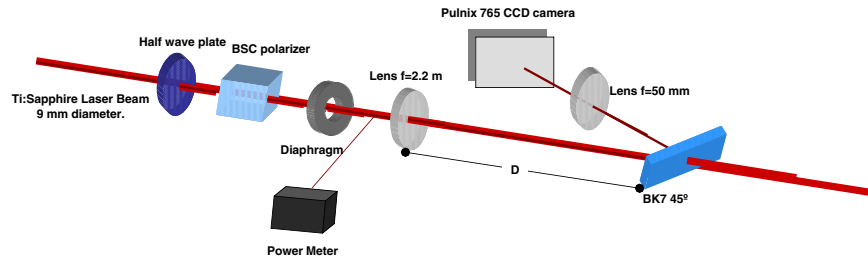


FIG. 1 (color online). Experimental setup: a Ti:Sa laser beam (790 nm, 120 fs) propagates through an aperture (5 mm diameter) and is focussed by a lens ($f = 2.2$ m). The pulse energy is selected by the combination of a $\lambda/2$ plate and a linear polarizer at adequate angles. After propagating through the focal point, the transversal beam profile is imaged using a BK7 plate and a CCD camera. Once the energy is measured, the power meter is removed from the path of the laser beam towards the BK7 plate.

transversal energy distribution of the beam is recorded by imaging the plate with a CCD camera. The appropriate control of the energy of the input beam is obtained with the combination of a variable angle $\lambda/2$ plate followed by a linear polarizer with fixed axis. The experiments were performed at 0.11 mJ and 0.56 mJ input energies (measured right after the aperture). In both cases the associated powers fall below the critical power for collapse due to Kerr self-focusing in air. This has been checked experimentally and also theoretically observing the propagation of the incident beam unmasked by the aperture [see Fig. 3(c) for the theoretical result]. The absence of any radiation channel or filament in this case rules out the possibility of collapse.

Our experimental results for the beam propagation after the focus are condensed in Fig. 2. Both plots outline the main features of the beam cross section found at different distances from the focusing lens. In particular, the radii corresponding to the widths at 25%, 50%, and 75% of the maximum energy detected by the CCD camera at different locations of the intercepting plate are presented. As a guide, we have delimited different shadowed areas to help to understand the figures. The white zones correspond, approximately, to radii where the beam intensity is lower than the 25% of the maximum. The different gray level zones, from lighter to darker, represent radii where the beam intensity is between 25% and 50%, between 50% and 75%, and above 75% of the maximum intensity. The insets correspond to the readout from the CCD camera at a particular position (≈ 460 cm). Figure 2(a) depicts the low energy case (0.11 mJ). The transversal energy distribution is found to be very close to the expected using the Fresnel diffraction formula, i.e., a ring structure that appears roughly 1 m after the focal spot and can be traced over 3 m before a new diffraction maximum appears at the center of the beam. In contrast, Fig. 2(b) corresponds to the higher energy case (0.56 mJ), and demonstrates completely different features: a pronounced maximum at the center of the beam followed by a more slow decay of the energy for the larger radii. This center structure is very similar to the one reported in [6] for a different propagating medium. It has been identified with a Townes soliton profile immersed in a background which corresponds to

the linear diffraction of the lower energy part of the pulse. A relevant aspect described in Fig. 2(b), and the central result of the present Letter, is the stability of this distribution over more than 1.5 m (about 31 Rayleigh lengths). The

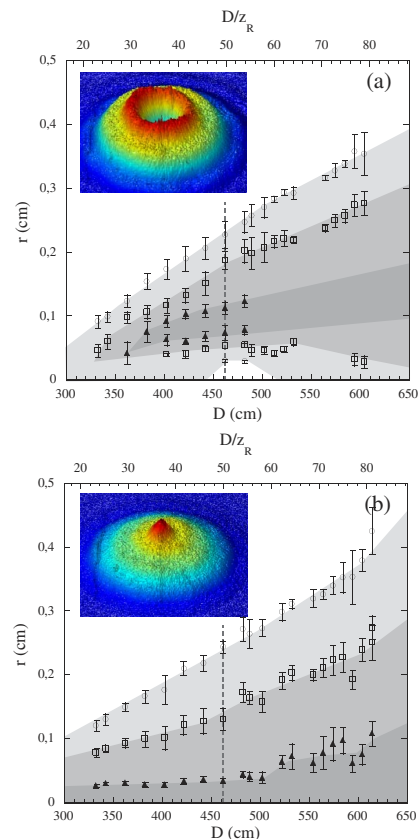


FIG. 2 (color online). Experimental beam profiles at different distances from the focusing lens for a 120 fs beam with energies of 0.11 (a) and 0.56 mJ (b), measured after the aperture. The data show the radii corresponding to 25% (circles), 50% (squares), and 75% (triangles) of the intensity maxima at every location. White zones correspond, approximately, to radii where the beam intensity is lower than the 25% of the maximum. The different gray level zones, from lighter to darker, represent radii where the beam intensity is between 25% and 50%, between 50% and 75%, and above 75% of the maximum intensity. The insets show the transversal beam profile at the distance marked by the dashed line.

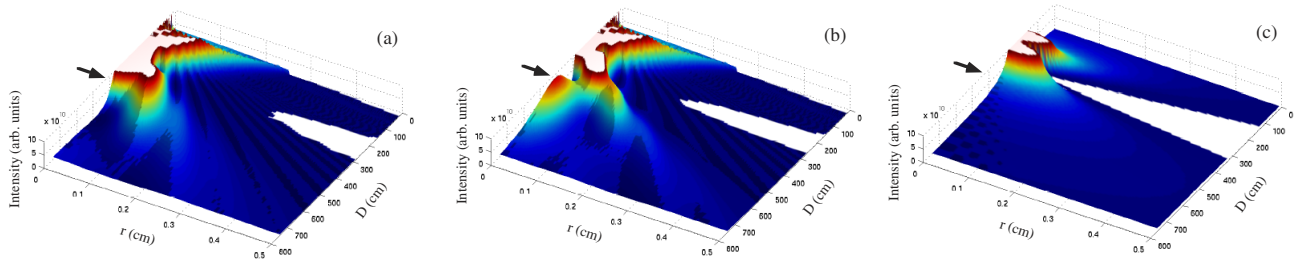


FIG. 3 (color online). Transversal field distributions computed from Eq. (1), for the same cases (a) and (b) as in Fig. 2. The black arrow marks the location of the Townes soliton. Plot (c) corresponds to the propagation of the beam in (b) without interposing the aperture.

stability of the beam channel in our results suggests that the central peak in the energy distribution is rather close to the actual Townes soliton profile. This result corresponds to a self-guiding situation in which an appreciable fraction of the beam energy propagates in a central channel with a radius of some hundreds of microns (a situation similar to the filamentation in air with higher intensities).

Further confirmation of the above interpretation can be drawn from the numerical integration of Eq. (1) with the initial conditions appropriate to describe the aperture-lens system. As noted above, this equation describes the propagation of a time slice of the electromagnetic pulse. We have chosen, therefore, to investigate the dynamics of the slice corresponding to the maximum intensity. Figures 3(a) and 3(b) show the computed energy distributions for the same cases as in Fig. 2. In the lower energy case, the central part of the beam after the focal point is rapidly depleted, forming the Fresnel diffraction ring. In correspondence with the experimental finding, the higher energy case [Fig. 3(b)] shows a central maximum (marked with an arrow) which decays after one or two meters. While the experimental and theoretical results agree quantitatively in the case of lowest energy, the agreement for 0.56 mJ is only qualitative. In this latter case, while the soliton structure is well described, the low intensity pattern around the soliton seems to be dependent on the temporal pulse shape. Since the theoretical model describes only one temporal slice at maximum power, this surrounding region is not accounted. We have to point out here that we have obtained this stable soliton solution with two different laser beams, each one with a different temporal shape. This probes the robustness of our scheme and demonstrates that, although the temporal envelope may affect the intensity distribution surrounding the soliton structure, it does not affect the soliton itself.

To retrieve the CCD readout from the theoretical point of view, one has to integrate the computations for different time slides accordingly to the actual temporal shape of the pulse. Unfortunately, in our case we have access only to the pulse autocorrelation information, which gives indirect information about the pulse shape. Our checks assuming an ideal Gaussian temporal profile do not provide a quantitative agreement satisfactory enough.

In [6], the identification of the Townes profile is obtained by best fit of the structure central maximum with the actual

profile of the soliton. Our numerical calculations permit us to be slightly more rigorous. The Townes soliton corresponds to a localized eigenstate of Eq. (1): $U_t(r, z) = \sqrt{I_t(r)} \exp(-ip_t z)$. If we express $U(r, z) = \sqrt{I(r, z)} \times \exp[i\phi(r, z)]$ as the central peak of the solution of Eq. (1) plotted in Fig. 3(b), the assimilation with the soliton requires: $I(r, z) \approx I_t(r)$ and $\partial\phi(r, z)/\partial z \approx p_t$ (constant). The first condition implies $I(r, z)$ localized and to follow a self-similar evolution in z [6]. The localization of the central maximum in Fig. 3(b) is evident, and the self-similarity along the z coordinate has been found in good approximation. The second condition, i.e., the eigenstate nature, can be considered as the fundamental test. Figure 4(a) shows $\partial\phi(r, z)/\partial z$ for the nonlinear case of Fig. 3(b). The arrow

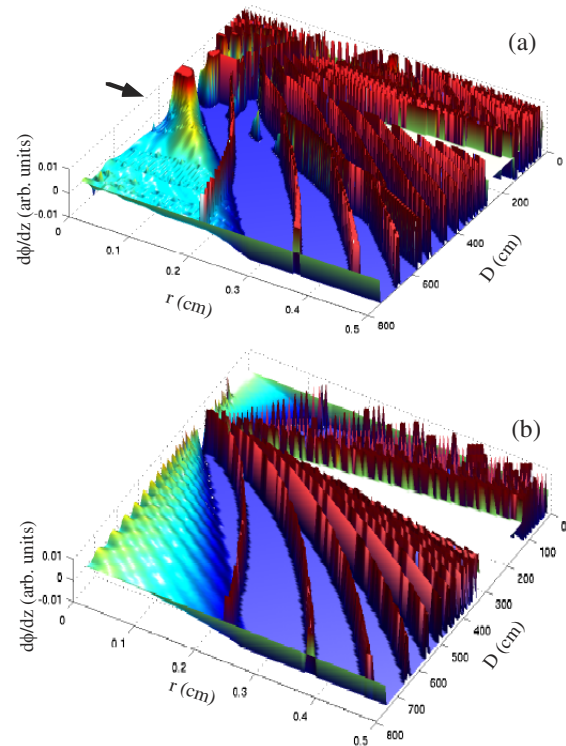


FIG. 4 (color online). Distribution of the derivative of the field phase along the propagation direction, $\partial\phi(r, z)/\partial z$, for the nonlinear cases with aperture [Fig. 3(b)] (a) and without aperture [Fig. 3(c)] (b).

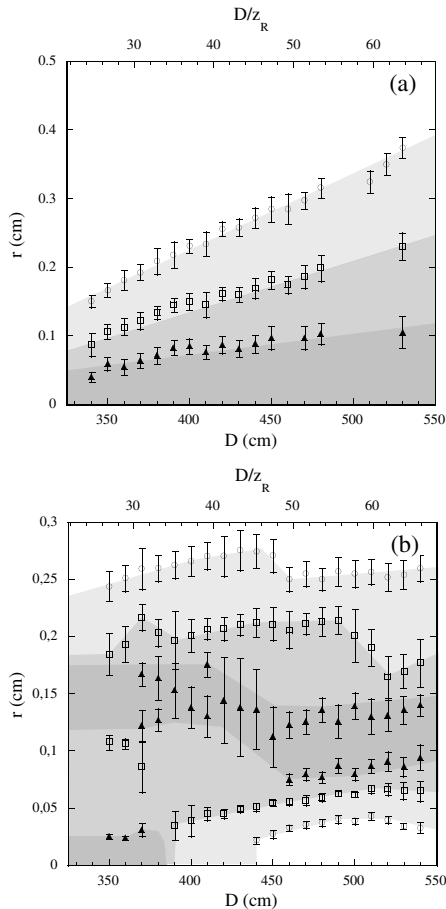


FIG. 5. Experimental beam profiles for a 120 fs laser beam of 0.56 mJ with the focusing lens and without the aperture (a) and with the aperture and without the focusing lens (b). The data show again the radii corresponding to 25% (circles), 50% (squares), and 75% (triangles) of the maximum of the intensity at every location. Shaded areas correspond to the same regions as in Fig. 2.

indicates the position of the maximum of the central energy distribution. The flatness of the surface indicates that the condition $\partial\phi(r, z)/\partial z \approx p_t$ is well attained in the region where the central structure is defined.

As commented before, the stability of the soliton solution reflects a very subtle balance between diffraction dispersion and Kerr self-focusing. Hence, the final achievement of a self-trapped solution depends fundamentally on the initial conditions (amplitude and phase distribution) of the field. In our case, the diffraction pattern generated by the aperture seems to be of fundamental importance. To show that this is indeed the case, we have performed experiments and simulations of the case corresponding to the 0.56 mJ focused beam removing the aperture [see Figs. 5(a) and 3(c), respectively]. Besides, we have also studied experimentally the propagation for the case of the aperture only [see Fig. 5(b)]. Note, that, for the first case, as the field is not screened, the initial beam profile is now

Gaussian with a sensibly higher energy. In this case the beam expansion after the focal point does not lead to a channel structure, and has the same characteristics as the theoretical plotted in Fig. 3(c). On the other hand, the phase distribution does not permit the identification of a single eigenstate, as becomes apparent in Fig. 4(b). For the case of removing the lens and leaving only the aperture we have obtained the typical Fresnel propagation with the appearance of ring structures [Fig. 5(b)]. These final figures confirm that the stable soliton solution appears due to the particular combination of the diffraction and the nonlinear effects.

We have reported the spontaneous generation of a narrow channel of radiation in the propagation of a short electromagnetic pulse in air, for energies below the energy threshold in which ionized filaments are possible. We have identified this channel (which extends over more than 1.5 m) as a structure that approximates closely to a Townes soliton, hence particularly stable. We believe that the enormous increase on the stability of the Townes soliton described in this Letter, even under a shot-to-shot fluctuating media as is air, demonstrates the robustness of the experimental procedure that has been used and opens new possibilities for their manipulation.

This work has been partially supported by the Spanish Ministerio de Ciencia y Tecnología (FEDER funds, Grant No. BFM2002-00033) and by the Junta de Castilla y León (Grant No. SA026A05). We are grateful to *VisionLab* Salamanca for its spirit of collaboration.

-
- [1] A. Braun *et al.*, *Opt. Lett.* **20**, 73 (1995).
 - [2] A critical point of view about this mechanism can be found in A. Dubietis *et al.*, *Phys. Rev. Lett.* **92**, 253903 (2004). The role of the background radiation in the stability of the filament is discussed in S. L. Chin, *Laser Phys.* (to be published).
 - [3] A. Couairon *et al.*, *J. Opt. Soc. Am. B* **19**, 1117 (2002).
 - [4] In our case, the laser pulse is composed of about 45 cycles, what makes SVEA still a reasonable approach [3]. Note, however, that for larger intensities the steep gradients in the refraction index associated with the plasma formation may invalidate this approximation (see the same reference).
 - [5] R. Y. Chiao, E. Garmine, and C. H. Townes, *Phys. Rev. Lett.* **13**, 479 (1964).
 - [6] K. D. Moll, A. L. Gaeta, and G. Fibich, *Phys. Rev. Lett.* **90**, 203902 (2003).
 - [7] Schemes for stabilizing these solitons through modifications in the nonlinear terms may be found in I. Towers and B. A. Malomed, *J. Opt. Soc. Am. B* **19**, 537 (2002) and G. D. Montesinos, V. M. Pérez-García, and H. Michinel, *Phys. Rev. Lett.* **92**, 133901 (2004).
 - [8] This is the main difference with the traditional filaments. These ones cannot be optically controlled due to the presence of a plasma.